VOL. 14, NO. 15, AUGUST 2019 ISSN 1819-6608
ARPN Journal of Engineering and Applied Sciences

www.arpnjournals.com

# EFFECT OF NON-HOMOGENEITY WITH THICKNESS AND TEMPERATURE VARIATION ON VIBRATION OF ORTHOTROPIC PARALLELOGRAM PLATE WITH SIMPLY SUPPORTED EDGES

Ashish Kumar Sharma[1], Manoj Kumar Dhiman[1], Harminder Singh[2], Preeti Prashar[3] and Pooja Sharma[1]
[1]Department of Mathematics, IEC University, Solan (HP), India
[2]Department of Mathematics, Bhai Gurdas Degree College, Sangrur (PB), India
[3]Department of Mathematics, D.A.V. College (Lahore), Ambala (HR), India
E-Mail: m.manojdhiman@gmail.com

**ABSTRACT**

In present paper a mathematical model is constructed to study the natural vibration of orthotropic parallelogram plate under the effect of bi-linear thickness variation and parabolic temperature distribution in both directions. Density (due to non-homogeneity) of the plate is taken to be linear along one direction. The governing differential equation has been solved with the help of variables separation method. The approximated frequency equation is derived by using Rayleigh-Ritz method by two term deflection function. The frequency values for the first two modes of vibration have been calculated for a simply supported (SSSS) parallelogram plate for various values of aspect ratio, thermal gradient, skew angle and taper constants with the help of MAPLE (latest computational software).

**Keywords:** vibration, bi-parabolic thickness, orthotropic, non-homogeneity, parallelogram plate, thermal gradient.

## 1. INTRODUCTION

In engineering, the whole machines and designing structures encounters vibrations so we can't move further without thinking about the impact of vibration. The prerequisite to know the impact of temperature on visco-elastic plates of variable thickness has turned out to be vital with modernization of technology. Tapered Plates with uniform and non-uniform thickness and temperature are generally utilized in vehicle division, aeronautical field, construction industry and marine structures. Different analysts investigated the vibration of various plates (homogeneous or non-homogeneous) having variable thickness and (considering or not) temperature effect.

An extensive review on linear vibration of simply supported elliptical and circular plates has been given by Leissa and Narita [1], [2]. Tomar *et al*. [3] considered the effect of taper gradient in two dimensions on elastic plates, but not on visco-elastic plates. Again Tomar *et al*. [4] studied temperature effect on frequency of an rectangular orthotropic plate with variable thickness in one direction. Gupta *et al.* [5] analyzed vibration of visco-elastic parallelogram plate with parabolic thickness variation. Again Gupta *et al.* [6] studied the effect of parabolic thickness variations on vibration of visco-elastic orthotropic parallelogram plate. Jain *et al.* [7] analyzed free vibration of rectangular plates of parabolically varying thickness. Khanna et al. [8] studied the vibration of visco-elastic square plate with variable thickness and thermal gradient. Sharma *et al*. [9] presented the mathematical study on vibration of visco-elastic parallelogram plate.Khanna *et al.* [10] studied Analysis of free vibrations of visco-elastic square plate of variable thickness with temperature effect. Again Khanna et al. [11] analyzed mechanical vibration of visco-elastic plate with thickness variation. Sharma *et al*. [12] represented the effect of bi-parabolic thermal and thickness variation on vibration of visco-elastic orthotropic rectangular plate. Sharma *et al.* [13] studied free vibration of visco-elastic orthotropic rectangular plate with bi-parabolic thermal effect and bi-linear thickness variation. Khanna *et al*. [14] considered the bi-parabolic thermal effect on vibration of visco-elastic square plate. Sharma *et al*. [15] discussed vibrational study of square plate with thermal effect and circular variation in density. Khanna *et al.* [16] considered effect of thermal gradient on vibration of non-uniform visco-elastic rectangular plate. Shimon and Hurmuzlu [17] presented a theoretical and experimental study of advanced control methods to suppress vibrations in a small square plate subject to temperature Variations. Sharma and Dhiman [18] discussed vibration analysis of simply supported parallelogram plate with bi-dimensional thickness and temperature deviation. Sharma Amit [19] studied vibration of skew plate with circular variation in thickness and poisson's ratio.

The literature shows that significant work has been done on vibration of various plates with clamped (CCCC) boundary conditions. So, In present paper the authors have examined the bi-parabolic temperature deviation impact on the vibrations of non-homogeneous parallelogram plates with inconsistent linear thickness in two measurements with simply supported (SSSS) boundary conditions on all four edges. Due to temperature deviation, we assume that non homogeneity occurs in modulus of versatility. Frequency values for first two modes of vibration are calculated for different numerical values of tapering constant, non-homogeneity, thermal gradient and aspect ratio. Results are shown in the form of tables and graphs.

VOL. 14, NO. 15, AUGUST 2019 ISSN 1819-6608
ARPN Journal of Engineering and Applied Sciences



## 2. ANALYSIS OF THE MODEL AND SOLUTION

### 2.1 Material

The parallelogram plate R with skew angle θ and sides a, b be shown in Figure-1. The plate is taken to be orthotropic and non-uniform. The skew coordinates of parallelogram plate are:

$$\xi = x - y\tan\theta,\ \eta = y\sec\theta \tag{2.1}$$

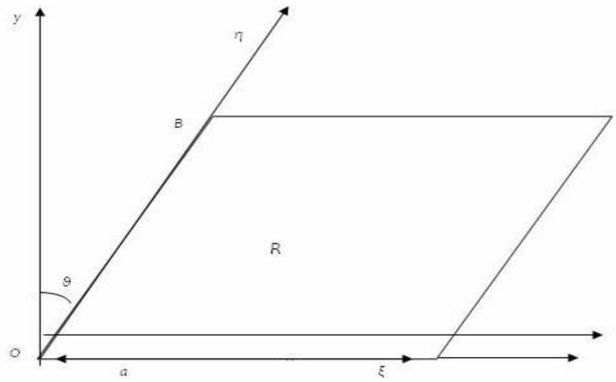


**Figure-1.** (The parallelogram plate R).

The plate considered here is subjected to parabolic temperature distribution along ξ- and η- directions, then

$$\tau = \tau_0(1 - \frac{\xi^2}{a^2})(1 - \frac{\eta^2}{b^2}) \tag{2.2}$$

where 'a' represents length, 'b' represents breadth and $\tau_0$ is temperature at origin of the plate. For orthotropic material, the temperature dependent modulus of elasticity is taken as:

$$E_\xi(\tau) = E_1\,(1 - \gamma\,\tau),\ E_\eta(\tau) = E_2\,(1 - \gamma\,\tau),$$
$$G_{\xi\eta}(\tau) = G_0\,(1 - \gamma\,\tau) \tag{2.3}$$

where $E_\xi$ and $E_\eta$ are Young's moduli in ξ- and η- directions respectively, $G_{\xi\eta}$ is shear modulus and γ is taken as slope variation of moduli with temperature. Using eqn. (2.2) in eqn. (2.3) one has

$$E_\xi(\tau) = E_1\left[1 - \alpha(1 - \frac{\xi^2}{a^2})(1 - \frac{\eta^2}{b^2})\right],$$
$$E_\eta(\tau) = E_2\left[1 - \alpha(1 - \frac{\xi^2}{a^2})(1 - \frac{\eta^2}{b^2})\right],$$
$$G_{\xi\eta}(\tau) = G_0\left[1 - \alpha(1 - \frac{\xi^2}{a^2})(1 - \frac{\eta^2}{b^2})\right] \tag{2.4}$$

Where $\alpha = \gamma\,\tau_0$, $(0 \le \alpha < 1)$ is thermal gradient.

The plate's thickness variation for the present study is to be assumed linearly in ξ- and η- directions which is represented by

$$h = h_0\left[\left(1 + \beta_1\frac{\xi}{a}\right)\left(1 + \beta_2\frac{\eta}{b}\right)\right] \tag{2.5}$$

Here $\beta_1$ and $\beta_2$ are known as tapering constants in ξ- and η- directions respectively and $h = h_0$ at $\xi, \eta = 0$.

The flexural rigidities $(D_\xi, D_\eta)$ and torsional rigidity $(D_{\xi\eta})$ of the plate are taken as:

$$D_\xi = \frac{E_\xi h^3}{12(1 - v_\xi v_\eta)},\ D_\eta = \frac{E_\eta h^3}{12(1 - v_\xi v_\eta)},\ D_{\xi\eta} = \frac{G_{\xi\eta} h^3}{12},$$
$$D_1 = v_\xi D_\eta = v_\eta D_\xi,\ H = D_1 + 2D_{\xi\eta} \tag{2.6}$$

Where $v_\xi$, $v_\eta$ are Poisson's ratios.

Using eqns. (2.4) and (2.5) in eqn. (2.6), we have

$$D_\xi = \frac{E_1 {h_0}^3}{12(1 - v_\xi v_\eta)}\left[\left\{1 - \alpha\left(1 - \frac{\xi^2}{a^2}\right)\left(1 - \frac{\eta^2}{b^2}\right)\right\}\left\{\left(1 + \beta_1\frac{\xi}{a}\right)\left(1 + \beta_2\frac{\eta}{b}\right)\right\}^3\right],$$
$$D_\eta = \frac{E_2 {h_0}^3}{12(1 - v_\xi v_\eta)}\left[\left\{1 - \alpha\left(1 - \frac{\xi^2}{a^2}\right)\left(1 - \frac{\eta^2}{b^2}\right)\right\}\left\{\left(1 + \beta_1\frac{\xi}{a}\right)\left(1 + \beta_2\frac{\eta}{b}\right)\right\}^3\right],$$
$$D_{\xi\eta} = \frac{G_0 {h_0}^3}{12}\left[\left\{1 - \alpha\left(1 - \frac{\xi^2}{a^2}\right)\left(1 - \frac{\eta^2}{b^2}\right)\right\}\left\{\left(1 + \beta_1\frac{\xi}{a}\right)\left(1 + \beta_2\frac{\eta}{b}\right)\right\}^3\right] \tag{2.7}$$

For non-homogeneous material, linear variation in density is taken as:

$$\rho = \rho_0\,(1 - c_1\frac{\xi}{a}) \tag{2.8}$$

where $c_1$ $(0 \le c_1 < 1)$ is non − homogeneity constant.

### 2.2 Boundary conditions

Boundary conditions for a non-homogeneous orthotropic (SSSS) parallelogram plate are taken as:

$$\left.\begin{array}{l} W = W_{,\xi\xi} = 0 \text{ at } \xi = 0, a \\ W = W_{,\eta\eta} = 0 \text{ at } \eta = 0, b \end{array}\right\} \tag{2.9}$$

Two-term deflection function to satisfy the boundary conditions, can be taken as:

$$W = \left[\left(\frac{\xi}{a}\right)\left(\frac{\eta}{b}\right)\left(1 - \frac{\xi}{a}\right)\left(1 - \frac{\eta}{b}\right)\right]$$
$$[A_1 + A_2\left(\frac{\xi}{a}\right)\left(\frac{\eta}{b}\right)\left(1 - \frac{\xi}{a}\right)\left(1 - \frac{\eta}{b}\right)] \tag{2.10}$$

where $A_1$, $A_2$ are constants to satisfy boundary conditions. Now, unit less variables having no dimension are using for our convince as:

$$E_1^* = \frac{E_1}{1 - v_\xi v_\eta},\ E_2^* = \frac{E_2}{1 - v_\xi v_\eta},\ E^* = v_\xi E_2^* = v_\eta E_1^* \tag{2.11}$$

ARPN Journal of Engineering and Applied Sciences



Components of $E_1^*$, $E_2^*$, $E^*$ and $G_0$ are $E_1^*$, $E_2^*\sec\theta$, $E^*\sec\theta$ and $G_0\sec\theta$ respectively in $\xi$- and $\eta$-directions. The expressions for strain energy ($V_E$) and kinetic energy ($T_E$) are taken as:

$$V_E = \frac{1}{2}\int_0^a\int_0^b \Big[D_\xi\left(W_{,\xi\xi}\right)^2 + D_\eta\left(W_{,\xi\xi}\tan^2\theta - 2W_{,\xi\eta}\sec\theta\tan\theta + W_{,\eta\eta}\sec^2\theta\right)^2 + 2D_1W_{,\xi\xi}(W_{,\xi\xi}\tan^2\theta + 2W_{,\xi\eta}\sec\theta\tan\theta + W_{,\eta\eta}\sec^2\theta) + 4D_{\xi\eta}\left(-W_{,\xi\xi}\tan\theta + W_{,\xi\eta}\sec\theta\right)^2\Big]\cos\theta\, d\eta d\xi \quad (2.12)$$

and

$$T_E = \frac{1}{2}\, p^2\int_0^a\int_0^b(\rho h W^2\cos\theta)d\eta d\xi \quad (2.13)$$

**2.3 Solution of frequency equation**

Rayleigh - Ritz technique is utilized to locate a suitable vibrational frequency. This technique chips away at the wonders that the maximum strain energy ($V_E$) must equal to maximum kinetic energy ($T_E$). An equation in the accompanying structure is acquired as:

$$\delta(V_E - T_E) = 0 \quad (2.14)$$

Using eqns. (2.7), (2.11) in eqn. (2.12) and (2.13), then substituting the values of $V_E$ and $T_E$ in eqn. (2.14), we obtained

$$\delta\left(V_E^* - \lambda^2 T_E^*\right) = 0 \quad (2.15)$$

Here,

$$V_E^* = \int_0^a\int_0^b\Big[\Big\{1-\alpha\left(1-\frac{\xi^2}{a^2}\right)\left(1-\frac{\eta^2}{b^2}\right)\Big\}\Big\{\left(1+\beta_1\frac{\xi}{a}\right)\left(1+\beta_2\frac{\eta}{b}\right)\Big\}^3\Big]\Big[\Big\{\cos^4\theta + \frac{E_2^*}{E_1^*}\sin^4\theta + 2\frac{E^*}{E_1^*}\sin^2\theta\cos^2\theta + 4\frac{G_0}{E_1^*}\sin^2\theta\cos^2\theta\Big\}W^2_{,\xi\xi} + \frac{E_2^*}{E_1^*}W^2_{,\eta\eta} + 4\Big\{\frac{E_2^*}{E_1^*}\sin^2\theta + \frac{G_0}{E_1^*}\cos^2\theta\Big\}W^2_{,\xi\eta} + 2\Big\{\frac{E_2^*}{E_1^*}\sin^2\theta + \frac{E^*}{E_1^*}\cos^2\theta\Big\}W_{,\xi\xi}W_{,\eta\eta} - 4\Big\{\frac{E_2^*}{E_1^*}\sin^3\theta + 2\frac{E^*}{E_1^*}\sin\theta\cos^2\theta + 2\frac{G_0}{E_1^*}\sin\theta\cos^2\theta\Big\}W_{,\xi\xi}W_{,\xi\eta} - 4\Big\{\frac{E_2^*}{E_1^*}\sin\theta\Big\}W_{,\eta\eta}W_{,\xi\eta}\Big]d\eta d\xi \quad (2.16)$$

$$T_E^* = \int_0^a\int_0^b[\left(1 - c_1\frac{\xi}{a}\right)\Big\{\left(1+\beta_1\frac{\xi}{a}\right)\left(1+\beta_2\frac{\eta}{b}\right)\Big\}]\, W^2\, d\eta d\xi \quad (2.17)$$

and frequency $\lambda^2 = \dfrac{12p^2\rho_0\, a^2\cos^5\theta}{E_1^*\, h_0^2}$

Now, the value of $A_1$ & $A_2$ is to be determined from (2.15) as

$$\frac{\partial(V_E^*-\lambda^2T_E^*)}{\partial A_s} = 0, \quad \text{for } s = 1, 2 \quad (2.18)$$

On solving equation (2.18), we have

$$m_{s1}A_1 + m_{s2}A_2 = 0, \quad \text{for } s = 1, 2 \quad (2.19)$$

Here $m_{s1}$, $m_{s2}$ (s = 1,2) comprises parametric constant and the frequency parameter. The determinant of the co-efficient of equation (2.19) must be zero, for non-trivial solution. We get the frequency equation as follows

$$\begin{vmatrix} m_{11} & m_{12} \\ m_{21} & m_{22} \end{vmatrix} = 0 \quad (2.20)$$

With the help of equation (2.20), we get quadratic equation in $\lambda^2$. We can obtain two roots of $\lambda^2$ from this equation. These roots give the first ($\lambda_1$) and second ($\lambda_2$) modes of vibration of frequency for various parameters of tapering constants, thermal gradient and aspect ratio for a simply supported plate.

**3. RESULT AND DISCUSSIONS**

The frequency ($\lambda$) for 1st and 2nd mode of vibration of an orthotropic (simply supported) parallelogram plate has been calculated for various values of thermal constant ($\alpha$), tapering constant ($\beta_1$ and $\beta_2$), aspect ratio (a/b) and non-homogeneity constant ($c_1$). All the results are obtained by using MAPLE software. Following parameters are used for these calculations [6]:

$\frac{E_2^*}{E_1^*} = 0.01$, $\frac{E^*}{E_1^*} = 0.3$, $\frac{G_0}{E_1^*} = 0.0333$, $\frac{E_1^*}{\rho} = 3.0 \times 10^5$, $h_0 = 0.01\text{m}$ and $\rho_0 = 0.345$

The results are given in Tables [1-4].

Table-1 represents thermal gradient ($\alpha$) versus frequency ($\lambda$) with fixed value of aspect ratio (a/b = 1) and different values of taper constants and non-homogeneity constant ($\beta_1 = \beta_2 = c_1$ = 0, 0.4, 0.8). It is apparent from Table-1 that as estimation of thermal gradient ($\alpha$) increments from 0 to 0.8 corresponding frequency value ($\lambda$) for 1st and 2nd mode of vibration decreases. It is also clear from Table-1 that the values of frequency increases for both modes as skew angle ($\theta$) varies from 30° to 60°.

ARPN Journal of Engineering and Applied Sciences



**Table-1.** Thermal Gradient (α) vs Frequency (λ).

| α | $\beta_1 = \beta_2 = c_1=0, \theta = 30^0$ | | $\beta_1 = \beta_2 = c_1=0.4, \theta = 45^0$ | | $\beta_1 = \beta_2 = c_1=0.8, \theta = 60^0$ | |
|---|---|---|---|---|---|---|
| | $\lambda_1$ | $\lambda_2$ | $\lambda_1$ | $\lambda_2$ | $\lambda_1$ | $\lambda_2$ |
| 0.0 | 11.18 | 101.84 | 15.15 | 137.63 | 18.73 | 167.55 |
| 0.2 | 10.57 | 97.51 | 14.48 | 133.73 | 18.04 | 164.12 |
| 0.4 | 9.93 | 92.97 | 13.78 | 129.71 | 17.48 | 160.63 |
| 0.6 | 9.24 | 88.21 | 13.03 | 125.56 | 16.58 | 157.05 |
| 0.8 | 8.49 | 83.17 | 12.24 | 121.27 | 15.79 | 153.39 |

Table-2.1 represents taper constant ($\beta_1$) versus Frequency (λ) with fixed value of aspect ratio (a/b = 1) and different values of thermal gradient, tapering constant and non-homogeneity ($\alpha = \beta_2 = c_1 = 0, 0.4, 0.8$).

From Table-2.1 it is clear that as value of tapering constant ($\beta_1$) varies from 0 to 0.8 corresponding frequency value (λ) also increases for 1st and 2nd mode of vibration.

**Table-2.1.** Taper Constant ($\beta_1$) vs Frequency (λ).

| $\beta_1$ | $\alpha = \beta_2 = c_1=0, \theta = 30^0$ | | $\alpha = \beta_2 = c_1=0.4, \theta = 45^0$ | | $\alpha = \beta_2 = c_1=0.8, \theta = 60^0$ | |
|---|---|---|---|---|---|---|
| | $\lambda_1$ | $\lambda_2$ | $\lambda_1$ | $\lambda_2$ | $\lambda_1$ | $\lambda_2$ |
| 0.0 | 11.18 | 101.84 | 11.03 | 101.40 | 9.83 | 88.88 |
| 0.2 | 12.33 | 113.01 | 12.38 | 114.77 | 11.29 | 103.40 |
| 0.4 | 13.52 | 125.78 | 13.78 | 129.71 | 12.77 | 119.22 |
| 0.6 | 14.73 | 139.73 | 15.20 | 145.76 | 14.28 | 135.97 |
| 0.8 | 15.98 | 154.53 | 16.64 | 162.61 | 15.79 | 153.39 |

Table-2.2 represents taper constant ($\beta_2$) versus Frequency (λ) with fixed value of aspect ratio (a/b = 1) and three different values of thermal gradient, tapering constants and non-homogeneity ($\alpha = \beta_1 = c_1 = 0, 0.4, 0.8$).

From Table-2.2 it is clear that as the value of tapering constant ($\beta_2$) varies from 0 to 0.8 corresponding value of frequency (λ) also increases for 1st and 2nd mode of vibration.

**Table-2.2.** Taper Constant ($\beta_2$) vs Frequency (λ).

| $\beta_2$ | $\alpha = \beta_1 = c_1=0, \theta = 30^0$ | | $\alpha = \beta_1 = c_1=0.4, \theta = 45^0$ | | $\alpha = \beta_1 = c_1=0.8, \theta = 60^0$ | |
|---|---|---|---|---|---|---|
| | $\lambda_1$ | $\lambda_2$ | $\lambda_1$ | $\lambda_2$ | $\lambda_1$ | $\lambda_2$ |
| 0.0 | 11.18 | 101.84 | 11.06 | 107.11 | 9.95 | 106.48 |
| 0.2 | 12.32 | 112.17 | 12.41 | 118.28 | 11.38 | 117.87 |
| 0.4 | 13.51 | 122.74 | 13.78 | 129.71 | 12.84 | 129.53 |
| 0.6 | 14.73 | 133.49 | 15.18 | 141.33 | 14.31 | 141.39 |
| 0.8 | 15.97 | 144.39 | 16.62 | 153.11 | 15.80 | 153.40 |

Table-3 represents non-homogeneity constant ($c_1$) versus frequency (λ) with fixed value of aspect ratio (a/b = 1) and different values of tapering constants and thermal constant ($\beta_1 = \beta_2 = \alpha = 0, 0.4, 0.8$). It is evident from Table-3 that as value of non-homogeneity constant ($c_1$) varies from 0 to 0.8 corresponding value of frequency (λ) also increases for 1st and 2nd mode of vibration.

ARPN Journal of Engineering and Applied Sciences



**Table-3.** Non-homogeneity constant ($c_1$) vs Frequency ($\lambda$).

| $c_1$ | $\alpha = \beta_1 = \beta_2=0, \theta = 30^0$ | | $\alpha = \beta_1 = \beta_2=0.4, \theta = 45^0$ | | $\alpha = \beta_1 = \beta_2=0.8, \theta = 60^0$ | |
|---|---|---|---|---|---|---|
| | $\lambda_1$ | $\lambda_2$ | $\lambda_1$ | $\lambda_2$ | $\lambda_1$ | $\lambda_2$ |
| 0.0 | 11.18 | 101.84 | 12.29 | 115.39 | 12.08 | 115.82 |
| 0.2 | 11.78 | 107.35 | 12.97 | 121.93 | 12.76 | 122.59 |
| 0.4 | 12.50 | 113.86 | 13.78 | 129.71 | 13.57 | 130.72 |
| 0.6 | 13.36 | 121.72 | 14.76 | 139.21 | 14.56 | 140.70 |
| 0.8 | 14.43 | 131.47 | 15.98 | 151.15 | 15.79 | 153.39 |

Table-4 represents aspect ratio (a/b) versus frequency ($\lambda$) with various values of tapering constants, thermal constant and non-homogeneity ($\beta_1 = \beta_2 = \alpha = c_1 = 0, 0.4, 0.8$). It is evident from Table-5 that as the value of aspect ratio increases from 0 to 1 corresponding value of frequency ($\lambda$) for 1st and 2nd mode of vibration decreases. It is also clear from Table-4 that the value of frequency increases for both modes as skew angle ($\theta$) varies from 30$^o$ to 60$^o$.

**Table-4.** Aspect ratio (a/b) vs Frequency ($\lambda$).

| a/b | $\alpha = \beta_1=\beta_2=0, c_1=0, \theta = 30^0$ | | $\alpha =\beta_1=\beta_2=0.4, c_1=0.4, \theta=45^0$ | | $\alpha =\beta_1=\beta_2=0.8, c_1=0.8, \theta=60^0$ | |
|---|---|---|---|---|---|---|
| | $\lambda_1$ | $\lambda_2$ | $\lambda_1$ | $\lambda_2$ | $\lambda_1$ | $\lambda_2$ |
| 0.2 | 267.70 | 2532.08 | 319.18 | 3216.48 | 334.56 | 3774.38 |
| 0.4 | 67.30 | 633.46 | 80.79 | 805.08 | 86.52 | 946.22 |
| 0.6 | 30.18 | 281.86 | 36.53 | 358.45 | 40.02 | 422.05 |
| 0.8 | 17.19 | 158.79 | 20.99 | 202.09 | 23.53 | 238.45 |
| 1.0 | 11.18 | 101.84 | 13.78 | 129.71 | 15.79 | 153.39 |

## 4. COMPARISON AND CONCLUSIONS

Rayleigh - Ritz technique is applied to study the effect of various parameters (taper constants, thermal constant, non-homogeneity constant, aspect ratio) on the vibration of non-homogeneous orthotropic parallelogram plates with linear thickness variation and parabolic temperature deviation in both directions. Authors compared the results obtained in case of non homogeneous material (SSSS boundary conditions) with homogeneous material (CCCC boundary conditions) at $c_1 = 0$ (non homogeneity parameter). Comparison tables for different values of taper constant ($\beta_1$) and aspect ratio (a/b) are:

**Table-5.1.** Taper Constant ($\beta_1$) vs Frequency ($\lambda$).

| $\beta_1$ | $\alpha = \beta_2 =0.4, c_1=0, \theta = 0^o$ | |
|---|---|---|
| | $\lambda_1$ | $\lambda_2$ |
| 0.0 | 14.05 {31.04} | 104.18 {124.88} |
| 0.2 | 14.95 {32.88} | 116.13 {135.03} |
| 0.4 | 15.92 {36.12} | 129.84 {146.11} |
| 0.6 | 16.94 {40.32} | 144.94 {158.88} |
| 0.8 | 18.00 {42.88} | 161.09 {172.08} |

**Table-5.2.** Aspect ratio (a/b) vs Frequency ($\lambda$).

| a/b | $\alpha = \beta_1=\beta_2=0, c_1=0, \theta = 30^0$ | |
|---|---|---|
| | $\lambda_1$ | $\lambda_2$ |
| 0.5 | 48.41 {26.52} | 442.32 {117.14} |
| 1.0 | 14.73 {39.22} | 114.52 {156.52} |
| 1.5 | 8.16 {67.08} | 54.23 {267.82} |
| 2.0 | 5.69 {109.12} | 33.54 {439.77} |
| 2.5 | 4.37 {163.88} | 24.30 {666.12} |

Here, the results of [9] are shown in { }. From Table-5.1 and Table-5.2 we can conclude that:

- Frequency values for both modes are less than that of [9] for same parameters.
- Frequency values are decreasing for both modes as we increased the values of aspect ratio in present study.

The authors also found that as the non-homogeneity increases in the material, the values for first and second mode of vibration (frequency value) also increases (as shown in Table-3). The frequency can be improved by taking reasonable variety in parameters. Therefore, the design engineers are advised to study the results of present paper before finalizing any structural design.

## REFERENCES

[1] Leissa A. W. 1967. Vibration of a simply supported elliptical plate. Journal of Sound and Vibration. 16: 145-148.

[2] Leissa A. W., Narita Y. 1980. Natural frequencies of a simply supported circular plate. Journal of Sound and Vibration. 70: 221-229.

[3] Tomar J. S., Gupta A. K. 1985. Effect of thermal gradient on frequencies of an orthotropic rectangular plate whose thickness varies in two directions. J.Sound and Vibration. 98: 257-262.

[4] Tomar J. S., Gupta A. K. 1983. Thermal effect on frequencies of an orthotropic rectangular plate of linearly varying thickness. J.Sound and Vibration. 90: 325-331.

[5] Gupta A. K., Kumar A., Gupta Y. K. 2010. Vibration of visco-elastic parallelogram plate with parabolic thickness variation. Applied Mathematics. 1(2): 128-136.

[6] Gupta A. K., Kumar Amit, Gupta D. V. 2012. Vibration of visco-elastic orthotropic parallelogram plate with parabolic thickness variations. International Journal of Engineering. 8(2): 61-70.

[7] Jain R. K., Soni S. R. 1973. Free vibration of rectangular plates of parabolically varying thickness. Indian Journal of Pure and Applied Mathematics. 4: 267-277.

[8] Khanna A., Sharma A. K. 2013. Natural Vibration of Visco-Elastic Plate of Varying Thickness with Thermal Effect. Journal of Applied Science and Engineering. 16(2): 135-140.

[9] Sharma S. K., Sharma A. K. 2015. Mathematical study on vibration of visco-elastic parallelogram plate. Mathematical Models in Engineering. 1(1): 12-19.

[10] Khanna A., Sharma A. K. 2012. A computational prediction on vibration of square plate by varying thickness with bi-dimensional thermal effect. International journal of emerging in engineering and development. 2(3): 191-196.

[11] Khanna A., Sharma A.K. 2012. Mechanical vibration of visco-elastic plate with thickness variation. Journal of Applied Mathematical Research. 1(2): 150-158.

[12] Sharma S. K., Sharma A.K. 2014. Effect of bi-parabolic thermal and thickness variation on vibration of visco-elastic orthotropic rectangular plate. Journal of Advanced Research in Manufacturing, Material Science and Metallurgical Engineering. 1(2): 26-28.

[13] Sharma A. K., Sharma S. K. 2014. Free vibration analysis of of visco-elastic orthotropic rectangular plate with bi-parabolic thermal effect and bi-linear thickness variation. Journal of Applied Mechanics and Computational Fluid Dynamics. 1(1): 10-23.

[14] Khanna A., Sharma A. K., Singh H., Mangotra V. K. 2011. Bi-parabolic thermal effect on vibration of visco-elastic square plate. Journal of applied Mathematics and Bioinformatics. 1(2): 39-48.

[15] Sharma A., Sharma A. K., Raghav A. K., Kumar V. 2016. Vibrational study of square plate with thermal effect and circular variation in density. Romanian Journal of Acoustics and Vibration. 13(2): 146-152.

[16] Khanna A., Kaur N. 2016. Effect of thermal gradient on vibration of non-uniform visco-elastic rectangular plate. Journal of The Institution of Engineers (India): Series C. 97( 2): 141 -148.

[17] Shimon P., Hurmuzlu Y. 2007. A theoretical and experimental study of advanced control methods to suppress vibrations in a small square plate subject to temperature Variations. Journal of Sound and Vibration. 302(2): 409-424.

[18] Sharma A. K., Dhiman M. K. 2018. Vibration analysis of simply supported parallelogram plate with bi-dimensional thickness and temperature deviation. International Journal of Research in Advent Technology. 6(12): 3711-3717.

[19] Sharma Amit. 2018. Vibration of skew plate with circular variation in thickness and poisson's ratio. Mechanics and Mechanical Engineering. 22(1): 49-58.